

Surface Collective Excitations in Ultrafast Pump–Probe Spectroscopy of Metal Nanoparticles

T. V. Shahbazyan and I. E. Perakis

Department of Physics and Astronomy, Vanderbilt University, Box 1807-B, Nashville, TN 37235

Abstract

The role of surface collective excitations in the electron relaxation in small metal particles is studied. It is shown that the dynamically screened electron–electron interaction in a nanoparticle contains a size–dependent correction induced by the surface. This leads to new channels of quasiparticle scattering accompanied by the emission of surface collective excitations. In noble–metal particles, the dipole collective excitations (surface plasmons) mediate a resonant scattering of d –holes to the conduction band. The role of this effect in the ultrafast optical dynamics of small nanoparticles is studied. With decreasing nanoparticle size, it leads to a drastic change in the differential absorption lineshape and a strong frequency dependence of the relaxation near the surface plasmon resonance. The experimental implications of these results in ultrafast pump–probe spectroscopy are addressed. We also discuss the size–dependence of conduction electron scattering rates.

I. INTRODUCTION

Surface collective excitations play an important role in the absorption of light by metal nanoparticles.^{1–5} In large particles with sizes comparable to the wave–length of light λ (but smaller than the bulk mean free path), the lineshape of the surface plasmon (SP) resonance is determined by the electromagnetic effects.¹ On the other hand, in small nanoparticles with radii $R \ll \lambda$, the absorption spectrum is governed by quantum confinement effects. For example, the momentum non–conservation due to the confining potential leads to the Landau damping of the SP and to a resonance linewidth inversely proportional to the nanoparticle size.^{1,6} Confinement also changes non–linear optical properties of nanoparticles: a size–dependent enhancement of the third–order susceptibilities, caused by the elastic surface scattering of single–particle excitations, has been reported.^{7–9}

Recently, extensive experimental studies of the electron relaxation in nanoparticles have been performed using ultrafast pump–probe spectroscopy.^{10–17} Unlike in semiconductors, the dephasing processes in metals are very fast, and nonequilibrium populations of optically excited electrons and holes are formed within several femtoseconds. These thermalize into the hot Fermi–Dirac distribution within several hundreds of femtoseconds, mainly due to e – e and h – h scattering.^{18–21} Since the electron heat capacity is much smaller than that of the lattice, a high electron temperature can be reached during less than 1 ps time scales, i.e., before any significant energy transfer to the phonon bath occurs. Note that in nanometer-sized

metal particles and nanoshells, the electron–phonon coupling is weaker than in the bulk.^{22,23} During this stage, the SP resonance has been observed to undergo a time–dependent spectral broadening.^{12,14} Subsequently, the electron and phonon baths equilibrate through the electron–phonon interactions over time intervals of a few picoseconds. During this incoherent stage, the hot electron distribution can be characterized by a time–dependent temperature.

The many–body correlations play an important role in the transient changes of the absorption spectrum.^{24–26} For example, in undoped materials, four–particle correlations and exciton–exciton interactions were shown to play a dominant role in the optical response for specific sequences of the optical pulses.^{27–29} Correlation effects also play an important role in doped systems.^{30,31} In nanoparticles, it has been shown that in order to explain the differential absorption lineshape, it is essential to take into account the *energy–dependent* e – e scattering of the optically–excited carriers near the Fermi surface.¹² Furthermore, despite the similarities to the bulk–like behavior, observed, e.g., in metal films, certain aspects of the optical dynamics in nanoparticles are significantly different.^{15,12,17} For example, experimental studies of small Cu nanoparticles revealed that the relaxation times of the pump–probe signal depend strongly on the probe frequency: the relaxation was considerably slower at the SP resonance.^{12,17} This and other observations suggest that collective surface excitations play an important role in the electron dynamics in small metal particles.

In this paper we address the role of surface collective excitations in the electron relaxation in small metal particles. We show that the dynamically screened e – e interaction contains a correction originating from the surface collective modes excited by an electron in nanoparticle. This opens up new quasiparticle scattering channels mediated by surface collective modes. We derive the corresponding scattering rates, which depend strongly on the nanoparticle size. The scattering rate of a conduction electron increases with energy, in contrast to the bulk–plasmon mediated scattering. In noble metal particles, we study the SP–mediated scattering of a d –hole into the conduction band. The scattering rate of this process depends strongly on temperature, and exhibits a *peak* as a function of energy due to the restricted phase space available for interband scattering. We show that this effect manifests itself in the ultrafast nonlinear optical dynamics of nanometer–sized particles. We perform self–consistent calculations of the temporal evolution of absorption spectrum in the presence of the pump pulse. For large sizes, the absorption peak exhibits a red shift at short time delays. We show that with decreasing size, the SP resonance develops a blue shift due to the SP–mediated interband scattering of the d –hole. We also find that the relaxation times of the pump–probe signal depend strongly on the probe frequency, in agreement with recent experiments.

The paper is organized as follows. In Section II we review the relevant basic relations of the linear response theory for nanoparticles. In Section III the dynamically screened Coulomb potential in a nanoparticle is derived. In Section IV we calculate the SP–mediated interband scattering rate of a d –band hole. In Section V we incorporate this effect in the calculation of the absorption coefficient. In Section VI we present our numerical results and discuss their experimental implications on the size and frequency dependence of the time–resolved pump–probe signal. In Section VII we study the quasiparticle scattering in the conduction band mediated by surface collective modes. Section VIII concludes the paper.

II. BASIC RELATIONS

In this section we recall the basic relations regarding the linear absorption by metal nanoparticles embedded in a medium with dielectric constant ϵ_m . We will focus primarily on noble metal particles containing several hundreds of atoms; in this case, the confinement affects the extended electronic states after the bulk lattice structure has been established. If the particles radii are small, $R \ll \lambda$, only dipole surface modes can be optically excited and non-local effects can be neglected. In this case the optical properties of this system are determined by the dielectric function¹

$$\epsilon_{\text{col}}(\omega) = \epsilon_m + 3p\epsilon_m \frac{\epsilon(\omega) - \epsilon_m}{\epsilon(\omega) + 2\epsilon_m}, \quad (1)$$

where $\epsilon(\omega) = \epsilon'(\omega) + i\epsilon''(\omega)$ is the dielectric function of a metal particle and $p \ll 1$ is the volume fraction occupied by nanoparticles in the colloid. Since the d -electrons play an important role in the optical properties of noble metals, the dielectric function $\epsilon(\omega)$ includes the interband contribution $\epsilon_d(\omega)$. For $p \ll 1$, the absorption coefficient of such a system is proportional to that of a single particle and is given by¹

$$\alpha(\omega) = -9p\epsilon_m^{3/2} \frac{\omega}{c} \text{Im} \frac{1}{\epsilon_s(\omega)}, \quad (2)$$

where

$$\epsilon_s(\omega) = \epsilon_d(\omega) - \omega_p^2 / \omega(\omega + i\gamma_s) + 2\epsilon_m, \quad (3)$$

plays the role of an effective dielectric function of a particle in the medium. Its zero, $\epsilon'_s(\omega_s) = 0$, determines the frequency of the SP, ω_s . In Eq. (3), ω_p is the bulk plasmon frequency of the conduction electrons, and the width γ_s characterizes the SP damping. The semiclassical result Eqs. (2) and (3) applies to nanoparticles with radii $R \gg q_{TF}^{-1}$, where q_{TF} is the Thomas-Fermi screening wave-vector ($q_{TF}^{-1} \sim 1 \text{ \AA}$ in noble metals). In this case, the electron density deviates from its classical shape only within a surface layer occupying a small fraction of the total volume.³² Quantum mechanical corrections, arising from the discrete energy spectrum, lead to a width $\gamma_s \sim v_F/R$, where $v_F = k_F/m$ is the Fermi velocity.^{1,6} Even though $\gamma_s/\omega_s \sim (q_{TF}R)^{-1} \ll 1$, this damping mechanism dominates over others, e.g., due to phonons, for sizes $R \lesssim 10 \text{ nm}$. In small clusters, containing several dozens of atoms, the semiclassical approximation breaks down and density functional or *ab initio* methods should be used.¹⁻⁴

It should be noted that, in contrast to surface collective excitations, the e - e scattering is not sensitive to the nanoparticle size as long as the condition $q_{TF}R \gg 1$ holds.³³ Indeed, for such sizes, the static screening is essentially bulk-like. At the same time, the energy dependence of the bulk e - e scattering rate,³⁴ $\gamma_e \propto (E - E_F)^2$, with E_F being the Fermi energy, comes from the phase-space restriction due to the momentum conservation, and involves the exchange of typical momenta $q \sim q_{TF}$. If the size-induced momentum uncertainty $\delta q \sim R^{-1}$ is much smaller than q_{TF} , the e - e scattering rate in a nanoparticle is not significantly affected by the confinement.³⁵

III. PLASMON-POLE APPROXIMATION IN SMALL METAL PARTICLES

In this section, we study the effect of the surface collective excitations on the e - e interactions in a spherical metal particle. To find the dynamically screened Coulomb potential, we generalize the method previously developed for calculations of local field corrections to the optical fields.³⁶ The potential $U(\omega; \mathbf{r}, \mathbf{r}')$ at point \mathbf{r} arising from an electron at point \mathbf{r}' is determined by the equation³⁷

$$U(\omega; \mathbf{r}, \mathbf{r}') = u(\mathbf{r} - \mathbf{r}') + \int d\mathbf{r}_1 d\mathbf{r}_2 u(\mathbf{r} - \mathbf{r}_1) \Pi(\omega; \mathbf{r}_1, \mathbf{r}_2) U(\omega; \mathbf{r}_2, \mathbf{r}'), \quad (4)$$

where $u(\mathbf{r} - \mathbf{r}') = e^2 |\mathbf{r} - \mathbf{r}'|^{-1}$ is the unscreened Coulomb potential and $\Pi(\omega; \mathbf{r}_1, \mathbf{r}_2)$ is the polarization operator. There are three contributions to Π , arising from the polarization of the conduction electrons, the d -electrons, and the medium surrounding the nanoparticles: $\Pi = \Pi_c + \Pi_d + \Pi_m$. It is useful to rewrite Eq. (4) in the “classical” form

$$\nabla \cdot (\mathbf{E} + 4\pi \mathbf{P}) = 4\pi e^2 \delta(\mathbf{r} - \mathbf{r}'), \quad (5)$$

where $\mathbf{E}(\omega; \mathbf{r}, \mathbf{r}') = -\nabla U(\omega; \mathbf{r}, \mathbf{r}')$ is the screened Coulomb field and $\mathbf{P} = \mathbf{P}_c + \mathbf{P}_d + \mathbf{P}_m$ is the electric polarization vector, related to the potential U as

$$\nabla \mathbf{P}(\omega; \mathbf{r}, \mathbf{r}') = -e^2 \int d\mathbf{r}_1 \Pi(\omega; \mathbf{r}, \mathbf{r}_1) U(\omega; \mathbf{r}_1, \mathbf{r}'). \quad (6)$$

In the random phase approximation, the intraband polarization operator is given by

$$\Pi_c(\omega; \mathbf{r}, \mathbf{r}') = \sum_{\alpha\alpha'} \frac{f(E_\alpha^c) - f(E_{\alpha'}^c)}{E_\alpha^c - E_{\alpha'}^c + \omega + i0} \psi_\alpha^c(\mathbf{r}) \psi_{\alpha'}^{c*}(\mathbf{r}) \psi_{\alpha'}^{c*}(\mathbf{r}') \psi_\alpha^c(\mathbf{r}'), \quad (7)$$

where E_α^c and ψ_α^c are the single-electron eigenenergies and eigenfunctions in the nanoparticle, and $f(E)$ is the Fermi-Dirac distribution (we set $\hbar = 1$). Since we are interested in frequencies much larger than the single-particle level spacing, $\Pi_c(\omega)$ can be expanded in terms of $1/\omega$. For the real part, $\Pi'_c(\omega)$, we obtain in the leading order³⁶

$$\Pi'_c(\omega; \mathbf{r}, \mathbf{r}_1) = -\frac{1}{m\omega^2} \nabla [n_c(\mathbf{r}) \nabla \delta(\mathbf{r} - \mathbf{r}_1)], \quad (8)$$

where $n_c(\mathbf{r})$ is the conduction electron density. In the following we assume, for simplicity, a step density profile, $n_c(\mathbf{r}) = \bar{n}_c \theta(R - r)$, where \bar{n}_c is the average density. The leading contribution to the imaginary part, $\Pi''_c(\omega)$, is proportional to ω^{-3} , so that $\Pi''_c(\omega) \ll \Pi'_c(\omega)$.

By using Eqs. (8) and (6), one obtains a familiar expression for \mathbf{P}_c at high frequencies,

$$\mathbf{P}_c(\omega; \mathbf{r}, \mathbf{r}') = \frac{e^2 n_c(\mathbf{r})}{m\omega^2} \nabla U(\omega; \mathbf{r}, \mathbf{r}') = \theta(R - r) \chi_c(\omega) \mathbf{E}(\omega; \mathbf{r}, \mathbf{r}'), \quad (9)$$

where $\chi_c(\omega) = -e^2 \bar{n}_c / m\omega^2$ is the conduction electron susceptibility. Note that, for a step density profile, \mathbf{P}_c vanishes outside the particle. The d -band and dielectric medium contributions to \mathbf{P} are also given by similar relations,

$$\mathbf{P}_d(\omega; \mathbf{r}, \mathbf{r}') = \theta(R - r) \chi_d(\omega) \mathbf{E}(\omega; \mathbf{r}, \mathbf{r}'), \quad (10)$$

$$\mathbf{P}_m(\omega; \mathbf{r}, \mathbf{r}') = \theta(r - R) \chi_m(\omega) \mathbf{E}(\omega; \mathbf{r}, \mathbf{r}'), \quad (11)$$

where $\chi_i = (\epsilon_i - 1)/4\pi$, $i = d, m$ are the corresponding susceptibilities and the step functions account for the boundary conditions.³⁸ Using Eqs. (9)–(11), one can write a closed equation for $U(\omega; \mathbf{r}, \mathbf{r}')$. Using Eq. (6), the second term of Eq. (4) can be presented as $-e^{-2} \int d\mathbf{r}_1 u(\mathbf{r} - \mathbf{r}_1) \nabla \cdot \mathbf{P}(\omega; \mathbf{r}_1, \mathbf{r}')$. Substituting the above expressions for \mathbf{P} , we then obtain after integrating by parts

$$\begin{aligned} \epsilon(\omega)U(\omega; \mathbf{r}, \mathbf{r}') &= \frac{e^2}{|\mathbf{r} - \mathbf{r}'|} + \int d\mathbf{r}_1 \nabla_1 \frac{1}{|\mathbf{r} - \mathbf{r}_1|} \cdot \nabla_1 [\theta(R - r)\chi(\omega) + \theta(r - R)\chi_m] U(\omega; \mathbf{r}_1, \mathbf{r}') \\ &\quad + i \int d\mathbf{r}_1 d\mathbf{r}_2 \frac{e^2}{|\mathbf{r} - \mathbf{r}_1|} \Pi_c''(\omega; \mathbf{r}_1, \mathbf{r}_2) U(\omega; \mathbf{r}_2, \mathbf{r}'), \end{aligned} \quad (12)$$

with

$$\epsilon(\omega) \equiv 1 + 4\pi\chi(\omega) = \epsilon_d(\omega) - \omega_p^2/\omega^2, \quad (13)$$

$\omega_p^2 = 4\pi e^2 \bar{n}_c/m$ being the plasmon frequency in the conduction band. The last term in the rhs of Eq. (12), proportional to $\Pi_c''(\omega)$, can be regarded as a small correction. To solve Eq. (12), we first eliminate the angular dependence by expanding $U(\omega; \mathbf{r}, \mathbf{r}')$ in spherical harmonics, $Y_{LM}(\hat{\mathbf{r}})$, with coefficients $U_{LM}(\omega; r, r')$. Using the corresponding expansion of $|\mathbf{r} - \mathbf{r}'|^{-1}$ with coefficients $Q_{LM}(r, r') = \frac{4\pi}{2L+1} r^{-L-1} r'^L$ (for $r > r'$), we get the following equation for $U_{LM}(\omega; r, r')$:

$$\begin{aligned} \epsilon(\omega)U_{LM}(\omega; r, r') &= Q_{LM}(r, r') + 4\pi [\chi(\omega) - \chi_m] \frac{L+1}{2L+1} \left(\frac{r}{R}\right)^L U_{LM}(\omega; R, r') \\ &\quad + ie^2 \sum_{L'M'} \int dr_1 dr_2 r_1^2 r_2^2 Q_{LM}(r, r_1) \Pi_{LM, L'M'}''(\omega; r_1, r_2) U_{L'M'}(\omega; r_2, r'), \end{aligned} \quad (14)$$

where

$$\Pi_{LM, L'M'}''(\omega; r_1, r_2) = \int d\hat{\mathbf{r}}_1 d\hat{\mathbf{r}}_2 Y_{LM}^*(\hat{\mathbf{r}}_1) \Pi_c''(\omega; \mathbf{r}_1, \mathbf{r}_2) Y_{L'M'}(\hat{\mathbf{r}}_2), \quad (15)$$

are the coefficients of the multipole expansion of $\Pi_c''(\omega; \mathbf{r}_1, \mathbf{r}_2)$. For $\Pi_c'' = 0$, the solution of Eq. (14) can be presented in the form

$$U_{LM}(\omega; r, r') = a(\omega)e^2 Q_{LM}(r, r') + b(\omega) \frac{4\pi e^2}{2L+1} \frac{r^L r'^L}{R^{2L+1}}, \quad (16)$$

with frequency-dependent coefficients a and b . Since $\Pi_c''(\omega) \ll \Pi_c'(\omega)$ for relevant frequencies, the solution of Eq. (14) in the presence of the last term can be written in the same form as Eq. (16), but with modified $a(\omega)$ and $b(\omega)$. Substituting Eq. (16) into Eq. (14), we obtain after lengthy algebra in the lowest order in Π_c''

$$a(\omega) = \epsilon^{-1}(\omega), \quad b(\omega) = \epsilon_L^{-1}(\omega) - \epsilon^{-1}(\omega), \quad (17)$$

where

$$\epsilon_L(\omega) = \frac{L}{2L+1} \epsilon(\omega) + \frac{L+1}{2L+1} \epsilon_m + i\epsilon_{cL}''(\omega), \quad (18)$$

is the effective dielectric function, whose zero, $\epsilon'_L(\omega_L) = 0$, determines the frequency of the collective surface excitation with angular momentum L ,¹

$$\omega_L^2 = \frac{L\omega_p^2}{L\epsilon'_d(\omega_L) + (L+1)\epsilon_m}. \quad (19)$$

In Eq. (18), $\epsilon''_{cL}(\omega)$ characterizes the damping of the L -pole collective mode by single-particle excitations, and is given by

$$\epsilon''_{cL}(\omega) = \frac{4\pi^2 e^2}{(2L+1)R^{2L+1}} \sum_{\alpha\alpha'} |M_{\alpha\alpha'}^{LM}|^2 [f(E_\alpha^c) - f(E_{\alpha'}^c)] \delta(E_\alpha^c - E_{\alpha'}^c + \omega), \quad (20)$$

where $M_{\alpha\alpha'}^{LM}$ are the matrix elements of $r^L Y_{LM}(\hat{\mathbf{r}})$. Due to the momentum nonconservation in a nanoparticle, the matrix elements are finite, which leads to the size-dependent width of the L -pole mode:^{6,36}

$$\gamma_L = \frac{2L+1}{L} \frac{\omega^3}{\omega_p^2} \epsilon''_{cL}(\omega). \quad (21)$$

For $\omega \sim \omega_L$, one can show that the width, $\gamma_L \sim v_F/R$, is independent of ω . Note that, in noble metal particles, there is an additional d -electron contribution to the imaginary part of $\epsilon_L(\omega)$ at frequencies above the onset Δ of the interband transitions.

Putting everything together, we arrive at the following expression for the dynamically-screened interaction potential in a nanoparticle:

$$U(\omega; \mathbf{r}, \mathbf{r}') = \frac{u(\mathbf{r} - \mathbf{r}')}{\epsilon(\omega)} + \frac{e^2}{R} \sum_{LM} \frac{4\pi}{2L+1} \frac{1}{\tilde{\epsilon}_L(\omega)} \left(\frac{rr'}{R^2} \right)^L Y_{LM}(\hat{\mathbf{r}}) Y_{LM}^*(\hat{\mathbf{r}}'), \quad (22)$$

with $\tilde{\epsilon}_L^{-1}(\omega) = \epsilon_L^{-1}(\omega) - \epsilon^{-1}(\omega)$. Equation (22), which is the main result of this section, represents a generalization of the plasmon pole approximation to spherical particles. The two terms in the rhs describe two distinct contributions. The first comes from the usual bulk-like screening of the Coulomb potential. The second contribution describes a new effective e - e interaction induced by the *surface*: the potential of an electron inside the nanoparticle excites high-frequency surface collective modes, which in turn act as image charges that interact with the second electron. It should be emphasized that, unlike in the case of the optical fields, the surface-induced dynamical screening of the Coulomb potential is *size-dependent*.

Note that the excitation energies of the surface collective modes are lower than the bulk plasmon energy, also given by Eq. (19) but with $\epsilon_m = 0$. This opens up new channels of quasiparticle scattering, considered in the next section.

IV. INTERBAND SCATTERING MEDIATED BY SURFACE PLASMONS

We now turn to the interband processes in noble metal particles and consider the scattering of a d -hole into the conduction band. We restrict ourselves to the scattering via the dipole channel, mediated by the SP. The corresponding surface-induced potential, given by the $L = 1$ term in Eq. (22), has the form

$$U_s(\omega; \mathbf{r}, \mathbf{r}') = \frac{3e^2}{R} \frac{\mathbf{r} \cdot \mathbf{r}'}{R^2} \frac{1}{\epsilon_s(\omega)}. \quad (23)$$

With this potential, the d -hole Matsubara self-energy is given by³⁷

$$\Sigma_\alpha^d(i\omega) = -\frac{3e^2}{R^3} \sum_{\alpha'} |\mathbf{d}_{\alpha\alpha'}|^2 \frac{1}{\beta} \sum_{i\omega'} \frac{G_{\alpha'}^c(i\omega' + i\omega)}{\epsilon_s(i\omega')}, \quad (24)$$

where $\mathbf{d}_{\alpha\alpha'} = \langle c, \alpha | \mathbf{r} | d, \alpha' \rangle = \langle c, \alpha | \mathbf{p} | d, \alpha' \rangle / im(E_\alpha^c - E_{\alpha'}^d)$ is the interband transition matrix element. Since the final state energies in the conduction band are high (in the case of interest here, they are close to the Fermi level), the matrix element can be approximated by the bulk-like expression $\langle c, \alpha | \mathbf{p} | d, \alpha' \rangle = \delta_{\alpha\alpha'} \langle c | \mathbf{p} | d \rangle \equiv \delta_{\alpha\alpha'} \mu$, the corrections due to surface scattering being suppressed by a factor of $(k_F R)^{-1} \ll 1$. After performing the frequency summation, we obtain for $\text{Im}\Sigma_\alpha^d$

$$\text{Im}\Sigma_\alpha^d(\omega) = -\frac{9e^2\mu^2}{m^2(E_\alpha^{cd})^2 R^3} \text{Im} \frac{N(E_\alpha^c - \omega) + f(E_\alpha^c)}{\epsilon_s(E_\alpha^c - \omega)}, \quad (25)$$

with $E_\alpha^{cd} = E_\alpha^c - E_\alpha^d$. We see that the scattering rate of a d -hole with energy E_α^d , $\gamma_h^s(E_\alpha^d) = \text{Im}\Sigma_\alpha^d(E_\alpha^d)$, has a strong R^{-3} dependence on the nanoparticle size.

The important feature the interband SP-mediated scattering rate is its energy dependence. Since the surface-induced potential, Eq. (23), allows for only vertical (dipole) interband single-particle excitations, the phase space for the scattering of a d -hole with energy E_α^d is restricted to a single final state in the conduction band with energy E_α^c . As a result, the d -hole scattering rate, $\gamma_h^s(E_\alpha^d)$, exhibits a *peak* as the difference between the energies of final and initial states, $E_\alpha^{cd} = E_\alpha^c - E_\alpha^d$, approaches the SP frequency ω_s [see Eq. (25)].

As we show in the next section, the fact that the scattering rate of a d -hole is dominated by the SP resonance, affects strongly the nonlinear optical dynamics in small nanoparticles. This is the case, in particular, when the SP frequency, ω_s , is close to the onset of interband transitions, Δ , as, e.g., in Cu and Au nanoparticles.^{1,12,14,16} Consider an e - h pair with excitation energy ω close to Δ . As we discussed, the d -hole can scatter into the conduction band by emitting a SP. According to Eq. (25), for $\omega \sim \omega_s$, this process will be resonantly enhanced. At the same time, the electron can scatter in the conduction band via the usual two-quasiparticle process. For $\omega \sim \Delta$, the electron energy is close to E_F , and its scattering rate is estimated as³⁹ $\gamma_e \sim 10^{-2}$ eV. Using the bulk value of μ , $2\mu^2/m \sim 1$ eV near the L-point,⁴⁰ we find that γ_h^s exceeds γ_e for $R \lesssim 2.5$ nm. In fact, one would expect that, in nanoparticles, μ is larger than in the bulk due to the localization of the conduction electron wave-functions.¹

V. SURFACE PLASMON OPTICAL DYNAMICS

In this section, we study the effect of the SP-mediated *interband* scattering on the nonlinear optical dynamics in noble metal nanoparticles. When the hot electron distribution has already thermalized and the electron gas is cooling to the lattice, the transient response of a nanoparticle can be described by the time-dependent absorption coefficient $\alpha(\omega, t)$,

given by Eq. (2) with time-dependent temperature.⁴¹ In noble-metal particles, the temperature dependence of α originates from two different sources. First is the phonon-induced correction to γ_s , which is proportional to the *lattice* temperature $T_l(t)$. As mentioned in the Introduction, for small nanoparticles this effect is relatively weak. Second, near the onset of the interband transitions, Δ , the absorption coefficient depends on the *electron* temperature $T(t)$ via the interband dielectric function $\epsilon_d(\omega)$ [see Eqs. (2) and (3)]. In fact, in Cu or Au nanoparticles, ω_s can be tuned close to Δ , so the SP damping by *interband* e - h excitations leads to an additional broadening of the absorption peak.¹ In this case, the temperature dependence of $\epsilon_d(\omega)$ dominates the pump-probe dynamics. Below we show that, near the SP resonance, both the temperature and frequency dependence of $\epsilon_d(\omega) = 1 + 4\pi\chi_d(\omega)$ are strongly affected by the SP-mediated interband scattering.

For non-interacting electrons, the interband susceptibility, $\chi_d(i\omega) = \tilde{\chi}_d(i\omega) + \tilde{\chi}_d(-i\omega)$, has the standard form³⁷

$$\tilde{\chi}_d(i\omega) = - \sum_{\alpha} \frac{e^2 \mu^2}{m^2 (E_{\alpha}^{cd})^2} \frac{1}{\beta} \sum_{i\omega'} G_{\alpha}^d(i\omega') G_{\alpha}^c(i\omega' + i\omega), \quad (26)$$

where $G_{\alpha}^d(i\omega')$ is the Green function of a d -electron. Since the d -band is fully occupied, the only allowed SP-mediated interband scattering is that of the d -hole. We assume here, for simplicity, a dispersionless d -band with energy E^d . Substituting $G_{\alpha}^d(i\omega') = [i\omega' - E^d + E_F - \Sigma_{\alpha}^d(i\omega')]^{-1}$, with $\Sigma_{\alpha}^d(i\omega)$ given by Eq. (24), and performing the frequency summation, we obtain

$$\tilde{\chi}_d(\omega) = \frac{e^2 \mu^2}{m^2} \int \frac{dE^c g(E^c)}{(E^{cd})^2} \frac{f(E^c) - 1}{\omega - E^{cd} + i\gamma_h^s(\omega, E^c)}, \quad (27)$$

where $g(E^c)$ is the density of states of conduction electrons. Here $\gamma_h^s(\omega, E^c) = \text{Im}\Sigma^d(E^c - \omega)$ is the scattering rate of a d -hole with energy $E^c - \omega$, for which we obtain from Eq. (25),

$$\gamma_h^s(\omega, E^c) = - \frac{9e^2 \mu^2}{m^2 (E^{cd})^2 R^3} f(E^c) \text{Im} \frac{1}{\epsilon_s(\omega)}, \quad (28)$$

where we neglected $N(\omega)$ for frequencies $\omega \sim \omega_s \gg k_B T$. Remarkably, $\gamma_h^s(\omega, E^c)$ exhibits a sharp peak as a function of the *frequency of the probe optical field*. The reason for this is that the scattering rate of a d -hole with energy E depends explicitly on the *difference* between the final and initial states, $E^c - E$, as discussed in the previous section: therefore, for a d -hole with energy $E = E^c - \omega$, the dependence on the final state energy, E^c , cancels out in $\epsilon_s(E^c - E)$ [see Eq. (25)]. This implies that the optically-excited d -hole experiences a *resonant scattering* into the conduction band as the probe frequency ω approaches the SP frequency. It is important to note that $\gamma_h^s(\omega, E^c)$ is, in fact, proportional to the absorption coefficient $\alpha(\omega)$ [see Eq. (2)]. Therefore, the calculation of the absorption spectrum is a *self-consistent* problem defined by Eqs. (2), (3), (27), and (28).

It should be emphasized that the effect of γ_h^s on $\epsilon_d''(\omega)$ *increases with temperature*. Indeed, the Fermi function in the rhs of Eq. (28) implies that γ_h^s is small unless $E^c - E_F \lesssim k_B T$. Since the main contribution to $\tilde{\chi}_d''(\omega)$ comes from energies $E^c - E_F \sim \omega - \Delta$, the d -hole scattering becomes efficient for electron temperatures $k_B T \gtrsim \omega_s - \Delta$. As a result, near the SP resonance, the time evolution of the differential absorption, governed by the temperature dependence of α , becomes strongly size-dependent, as we show in the next section.

VI. NUMERICAL RESULTS

In the numerical calculations below, we adopt the parameters of the experiment of Ref. 12, which was performed on $R \simeq 2.5$ nm Cu nanoparticles with SP frequency, $\omega_s \simeq 2.22$ eV, slightly above the onset of the interband transitions, $\Delta \simeq 2.18$ eV. In order to describe the time-evolution of the differential absorption spectra, we first need to determine the time-dependence of the electron temperature, $T(t)$, due to the relaxation of the electron gas to the lattice. For this, we employ a simple two-temperature model, defined by heat equations for $T(t)$ and the lattice temperature $T_l(t)$:

$$\begin{aligned} C(T) \frac{\partial T}{\partial t} &= -G(T - T_l), \\ C_l \frac{\partial T_l}{\partial t} &= G(T - T_l), \end{aligned} \quad (29)$$

where $C(T) = \Gamma T$ and C_l are the electron and lattice heat capacities, respectively, and G is the electron-phonon coupling.⁴² The parameter values used here were $G = 3.5 \times 10^{16}$ Wm⁻³K⁻¹, $\Gamma = 70$ Jm⁻³K⁻², and $C_l = 3.5$ Jm⁻³K⁻¹. The values of γ_s and μ were extracted from the fit to the linear absorption spectrum, and the initial condition for Eq. (29) was taken as $T_0 = 800$ K, the estimated pump-induced hot electron temperature.¹² We then self-consistently calculated the time-dependent absorption coefficient $\alpha(\omega, t)$, which describes the spectrum in the presence of the pump field. The differential transmission is then proportional to $\alpha_r(\omega) - \alpha(\omega, t)$, where $\alpha_r(\omega)$ is the absorption coefficient at the room temperature.

In Fig. 1 we show the calculated absorption spectra for different nanoparticle sizes. Fig. 1(a) shows the spectra at several time delays for $R = 5.0$ nm; for this size, the SP-mediated d -hole scattering has no effect. With decreasing nanoparticle size, the linear absorption spectra are not significantly altered, as can be seen in Figs. 1(b) and (c)]. However, the change becomes pronounced at short time delays corresponding to higher temperatures [see Figs. 1(b) and (c)]. This effect is clearly seen in the differential transmission spectra, shown in Fig. 2, which undergoes qualitative transformation with decreasing size.

Note that it is necessary to include the intraband e - e scattering in order to reproduce the differential transmission lineshape observed in the experiment.¹² For optically excited electron energy close to E_F , this can be achieved by adding the e - e scattering rate³⁴ $\gamma_e(E^c) \propto [1 - f(E^c)][(E^c - E_F)^2 + (\pi k_B T)^2]$ to γ_h^s in Eq. (27). The difference in $\gamma_e(E^c)$ for E^c below and above E_F leads to a lineshape similar to that expected from the combination of red-shift and broadening [see Fig. 2(a)].

In Figs. 2(b) and (c) we show the differential transmission spectra with decreasing nanoparticle size. For $R = 2.5$ nm, the apparent red-shift is reduced [see Fig. 2(b)]. This change can be explained as follows. Since here $\omega_s \sim \Delta$, the SP is damped by the interband excitations. This broadens the spectra for $\omega > \omega_s$, so that the absorption peak is *asymmetric*. The d -hole scattering with the SP enhances the damping; since the ω -dependence of γ_h^s follows that of α , this effect is larger above the resonance. On the other hand, the efficiency of the scattering increases with temperature, as discussed above. Therefore, for short time delays, the relative increase in the absorption is larger for $\omega > \omega_s$. With decreasing size, the strength of this effect increases further, leading to an apparent blue-shift [see Fig. 2(c)]. Such a strong change in the absorption dynamics originates from the R^{-3} dependence of the

d -hole scattering rate; reducing the size by the factor of two results in an enhancement of γ_h^s by an order of magnitude.

In Fig. 3 we show the time evolution of the differential transmission at several frequencies close to ω_s . It can be seen that the relaxation is slowest at the SP resonance; this characterizes the robustness of the collective mode, which determines the peak position, versus the single-particle excitations, which determine the resonance width. For larger sizes, at which γ_h^s is small, the change in the differential transmission decay rate with *frequency* is smoother above the resonance [see Fig. 3(a)]. This stems from the asymmetric lineshape of the absorption peak, mentioned above: the absorption is larger for $\omega > \omega_s$, so that its *relative* change with temperature is weaker. For smaller nanoparticle size, the decay rates become similar above and below ω_s [see Fig. 3(b)]. This change in the frequency dependence is related to the stronger SP damping for $\omega > \omega_s$ due to the d -hole scattering, as discussed above. Since this additional damping is reduced with decreasing temperature, the relaxation is faster above the resonance. This rather “nonlinear” relation between the time-evolution of the pump-probe signal and that of the temperature becomes even stronger for smaller sizes [see Fig. 3(c)]. In this case, the frequency dependence of the differential transmission decay below and above ω_s is reversed. Note that a frequency dependence consistent with our calculations presented in Fig. 3(b) was, in fact, observed in the experiment of Ref. 12, shown in Fig. 3(d).

VII. QUASIPARTICLE SCATTERING VIA SURFACE COLLECTIVE MODES

Let us now turn to the electron scattering in the conduction band accompanied by the emission of surface collective modes. In the first order in the surface-induced potential, given by the second term in the rhs of Eq. (22), the corresponding scattering rate can be obtained from the Matsubara self-energy³⁷

$$\Sigma_\alpha^c(i\omega) = -\frac{1}{\beta} \sum_{i\omega'} \sum_{LM} \sum_{\alpha'} \frac{4\pi e^2}{(2L+1)R^{2L+1}} \frac{|M_{\alpha\alpha'}^{LM}|^2}{\tilde{\epsilon}_L(i\omega')} G_{\alpha'}^c(i\omega' + i\omega), \quad (30)$$

where $G_\alpha^c = (i\omega - E_\alpha^c)^{-1}$ is the non-interacting Green function of the conduction electron. Here the matrix elements $M_{\alpha\alpha'}^{LM}$ are calculated with the one-electron wave functions $\psi_\alpha^c(\mathbf{r}) = R_{nl}(r)Y_{lm}(\hat{\mathbf{r}})$. Since $|\alpha\rangle$ and $|\alpha'\rangle$ are the initial and final states of the scattered electron, the main contribution to the L th term of the angular momentum sum in Eq. (30) will come from electron states with energy difference $E_\alpha - E_{\alpha'} \sim \omega_L$. Therefore, $M_{\alpha\alpha'}^{LM}$ can be expanded in terms of the small parameter $E_0/|E_\alpha^c - E_{\alpha'}^c| \sim E_0/\omega_L$, where $E_0 = (2mR^2)^{-1}$ is the characteristic confinement energy. The leading term can be obtained by using the following procedure.^{6,36} We present $M_{\alpha\alpha'}^{LM}$ as

$$M_{\alpha\alpha'}^{LM} = \langle c, \alpha | r^L Y_{LM}(\hat{\mathbf{r}}) | c, \alpha' \rangle = \frac{\langle c, \alpha | [H, [H, r^L Y_{LM}(\hat{\mathbf{r}})]] | c, \alpha' \rangle}{(E_\alpha^c - E_{\alpha'}^c)^2}, \quad (31)$$

where $H = H_0 + V(r)$ is the Hamiltonian of an electron in a nanoparticle with confining potential $V(r) = V_0\theta(r - R)$. Since $[H, r^L Y_{LM}(\hat{\mathbf{r}})] = -\frac{1}{m}\nabla[r^L Y_{LM}(\hat{\mathbf{r}})] \cdot \nabla$, the numerator in Eq. (31) contains a term proportional to the gradient of the confining potential, which peaks sharply at the surface. The corresponding contribution to the matrix element describes the

surface scattering of an electron making the L -pole transition between the states $|c, \alpha\rangle$ and $|c, \alpha'\rangle$, and gives the dominant term of the expansion. Thus, in the leading order in $|E_\alpha^c - E_{\alpha'}^c|^{-1}$, we obtain

$$M_{\alpha\alpha'}^{LM} = \frac{\langle c, \alpha | \nabla[r^L Y_{LM}(\hat{\mathbf{r}})] \cdot \nabla V(r) | c, \alpha' \rangle}{m(E_\alpha^c - E_{\alpha'}^c)^2} = \frac{LR^{L+1}}{m(E_\alpha^c - E_{\alpha'}^c)^2} V_0 R_{nl}(R) R_{n'l'}(R) \varphi_{lm, l'm'}^{LM}, \quad (32)$$

with $\varphi_{lm, l'm'}^{LM} = \int d\hat{\mathbf{r}} Y_{lm}^*(\hat{\mathbf{r}}) Y_{LM}(\hat{\mathbf{r}}) Y_{l'm'}(\hat{\mathbf{r}})$. Note that, for $L = 1$, Eq. (32) becomes exact. For electron energies close to the Fermi level, $E_{nl}^c \sim E_F$, the radial quantum numbers are large, and the product $V_0 R_{nl}(R) R_{n'l'}(R)$ can be evaluated by using semiclassical wave-functions. In the limit $V_0 \rightarrow \infty$, this product is given by⁶ $2\sqrt{E_{nl}^c E_{n'l'}^c}/R^3$, where $E_{nl}^c = \pi^2(n + l/2)^2 E_0$ is the electron eigenenergy for large n . Substituting this expression into Eq. (32) and then into Eq. (30), we obtain

$$\Sigma_\alpha^c(i\omega) = -\frac{1}{\beta} \sum_{i\omega'} \sum_L \sum_{n'l'} C_{ll'}^L \frac{4\pi e^2}{(2L+1)R} \frac{E_{nl}^c E_{n'l'}^c}{(E_{nl}^c - E_{n'l'}^c)^4} \frac{(4LE_0)^2}{\tilde{\epsilon}_L(i\omega')} G_{\alpha'}^c(i\omega' + i\omega), \quad (33)$$

with

$$C_{ll'}^L = \sum_{M, m'} |\varphi_{lm, l'm'}^{LM}|^2 = \frac{(2L+1)(2l'+1)}{8\pi} \int_{-1}^1 dx P_l(x) P_L(x) P_{l'}(x), \quad (34)$$

where $P_l(x)$ are Legendre polynomials; we used properties of the spherical harmonics in the derivation of Eq. (34). For $E_{nl}^c \sim E_F$, the typical angular momenta are large, $l \sim k_F R \gg 1$, and one can use the large- l asymptotics of P_l ; for the low multipoles of interest, $L \ll l$, the integral in Eq. (34) can be approximated by $\frac{2}{2l'+1} \delta_{ll'}$. After performing the Matsubara summation, we obtain for the imaginary part of the self-energy that determines the electron scattering rate

$$\text{Im} \Sigma_\alpha^c(\omega) = -\frac{16e^2}{R} E_0^2 \sum_L L^2 \int dE g_l(E) \frac{EE_\alpha^c}{(E_\alpha^c - E)^4} \text{Im} \frac{N(E - \omega) + f(E)}{\tilde{\epsilon}_L(E - \omega)}, \quad (35)$$

where $N(E)$ is the Bose distribution and $g_l(E)$ is the density of states of a conduction electron with angular momentum l ,

$$g_l(E) = 2 \sum_n \delta(E_{nl}^c - E) \simeq \frac{R}{\pi} \sqrt{\frac{2m}{E}}, \quad (36)$$

where we replaced the sum over n by an integral (the factor of 2 accounts for spin).

Each term in the sum in the rhs of Eq. (35) represents a channel of electron scattering mediated by a collective surface mode with angular momentum L . For low L , the difference between the energies of modes with successive values of L is larger than their widths, so that the different channels are well separated. Note that since all ω_L are smaller than the frequency of the (undamped) bulk plasmon, one can replace $\tilde{\epsilon}_L(\omega)$ by $\epsilon_L(\omega)$ in the integrand of Eq. (35) for frequencies $\omega \sim \omega_L$.

Consider now the $L = 1$ term in Eq. (35), which describes the SP-mediated scattering channel. The main contribution to the integral comes from the SP pole in $\epsilon_1^{-1}(\omega) = 3\epsilon_s^{-1}(\omega)$,

where $\epsilon_s(\omega)$ is the same as in Eq. (3). To estimate the scattering rate, we approximate $\text{Im}\epsilon_s^{-1}(\omega)$ by a Lorentzian,

$$\text{Im}\epsilon_s^{-1}(\omega) = -\frac{\gamma_s\omega_p^2/\omega^3 + \epsilon_d''(\omega)}{[\epsilon'(\omega) + 2\epsilon_m]^2 + [\gamma_s\omega_p^2/\omega^3 + \epsilon_d''(\omega)]^2} \simeq -\frac{\omega_s^2}{\epsilon_d'(\omega_s) + 2\epsilon_m} \frac{\omega_s\gamma}{(\omega^2 - \omega_s^2)^2 + \omega_s^2\gamma^2}, \quad (37)$$

where $\omega_s \equiv \omega_1 = \omega_p/\sqrt{\epsilon_d'(\omega_s) + 2\epsilon_m}$ and $\gamma = \gamma_s + \omega_s\epsilon_d''(\omega_s)$ are the SP frequency and width, respectively. For typical widths $\gamma \ll \omega_s$, the integral in Eq. (35) can be easily evaluated, yielding

$$\text{Im}\Sigma_\alpha^c(\omega) = -\frac{24e^2\omega_s E_0^2}{\epsilon_d'(\omega_s) + 2\epsilon_m} \frac{E_\alpha^c \sqrt{2m(\omega - \omega_s)}}{(\omega - E_\alpha^c - \omega_s)^4} [1 - f(\omega - \omega_s)]. \quad (38)$$

Finally, using the relation $e^2 k_F [\epsilon_d'(\omega_s) + 2\epsilon_m]^{-1} = 3\pi\omega_s^2/8E_F$, the SP-mediated scattering rate, $\gamma_e^s(E_\alpha^c) = -\text{Im}\Sigma_\alpha^c(E_\alpha^c)$, takes the form

$$\gamma_e^s(E) = 9\pi \frac{E_0^2}{\omega_s} \frac{E}{E_F} \left(\frac{E - \omega_s}{E_F} \right)^{1/2} [1 - f(E - \omega_s)]. \quad (39)$$

Recalling that $E_0 = (2mR^2)^{-1}$, we see that the scattering rate of a conduction electron is *size-dependent*: $\gamma_e^s \propto R^{-4}$. At $E = E_F + \omega_s$, the scattering rate jumps to the value $9\pi(1 + \omega_s/E_F)E_0^2/\omega_s$, and then *increases* with energy as $E^{3/2}$ (for $\omega_s \ll E_F$). This should be contrasted with the usual (bulk) plasmon-mediated scattering, originating from the first term in Eq. (22), with the rate decreasing as $E^{-1/2}$ above the onset.³⁷ To estimate the size at which γ_e^s becomes important, we should compare it with the Fermi liquid e - e scattering rate,³⁴ $\gamma_e(E) = \frac{\pi^2 q_{TF}}{16k_F} \frac{(E - E_F)^2}{E_F}$. For energies $E \sim E_F + \omega_s$, the two rates become comparable for

$$(k_F R)^2 \simeq 12 \frac{E_F}{\omega_s} \left(1 + \frac{E_F}{\omega_s} \right)^{1/2} \left(\frac{k_F}{\pi q_{TF}} \right)^{1/2}. \quad (40)$$

In the case of a Cu nanoparticle with $\omega_s \simeq 2.2$ eV, we obtain $k_F R \simeq 8$, which corresponds to the radius $R \simeq 3$ nm. At the same time, in this energy range, the width γ_e^s exceeds the mean level spacing δ , so that the energy spectrum is still continuous. The strong size dependence of γ_e^s indicates that, although γ_e^s increases with energy slower than γ_e , the SP-mediated scattering should dominate for nanometer-sized particles. Note that the size and energy dependences of scattering in different channels are similar. Therefore, the total scattering rate as a function of energy will represent a series of steps at the collective excitation energies $E = \omega_L < \omega_p$ on top of a smooth energy increase. We expect that this effect could be observed experimentally in time-resolved two-photon photoemission measurements of size-selected cluster beams.³⁹

VIII. CONCLUSIONS

To summarize, we have examined theoretically the role of size-dependent correlations in the electron relaxation in small metal particles. We identified a new mechanism of quasi-particle scattering, mediated by collective surface excitations, which originates from the

surface-induced dynamical screening of the e - e interactions. The behavior of the corresponding scattering rates with varying energy and temperature differs substantially from that in the bulk metal. In particular, in noble metal particles, the energy dependence of the d -hole scattering rate was found similar to that of the absorption coefficient. This led us to a self-consistent scheme for the calculation of the absorption spectrum near the surface plasmon resonance.

An important aspect of the SP-mediated scattering is its strong dependence on size. Our estimates show that it becomes comparable to the usual Fermi-liquid scattering in nanometer-sized particles. This size regime is, in fact, intermediate between “classical” particles with sizes larger than 10 nm, where the bulk-like behavior dominates, and very small clusters with only dozens of atoms, where the metallic properties are completely lost. Although the static properties of nanometer-sized particles are also size-dependent, the deviations from their bulk values do not change the qualitative features of the electron *dynamics*. In contrast, the size-dependent *many-body* effects, studied here, *do* affect the dynamics in a significant way during time scales comparable to the relaxation times. As we have shown, the SP-mediated interband scattering reveals itself in the transient pump-probe spectra. In particular, as the nanoparticle size decreases, the calculated time-resolved differential absorption develops a characteristic lineshape corresponding to a resonance blue-shift. At the same time, near the SP resonance, the scattering leads to a significant change in the frequency dependence of the relaxation time of the pump-probe signal, consistent with recent experiments. These results indicate the need for a systematic experimental studies of the size-dependence of the transient nonlinear optical response, as we approach the transition from boundary-constrained nanoparticles to molecular clusters.

This work was supported by NSF CAREER award ECS-9703453, and, in part, by ONR Grant N00014-96-1-1042 and by Hitachi Ltd.

REFERENCES

- ¹ See, e.g., U. Kreibig and M. Vollmer, *Optical Properties of Metal Clusters* (Springer, Berlin, 1995), and references therein.
- ² See, e.g., W. A. De Heer, Rev. Mod. Phys. **65**, 611 (1993).
- ³ See, e.g., M. Brack, Rev. Mod. Phys. **65**, 677 (1993).
- ⁴ See, e.g., *Physics and Chemistry of Finite Systems: From clusters to Crystals*, edited by P. Jena *et al.* (NATO Advanced Study Institute Series C, Kluwer Academic, Dordrecht/Boston, 1992).
- ⁵ C. Flytzanis, F. Hache, M. C. Klein, D. Ricard, and Ph. Roussignol, in *Progress in Optics XXIX*, edited by E. Wolf (Elsevier, Amsterdam, 1991) p. 321.
- ⁶ A. Kawabata and R. Kubo, J. Phys. Soc. Japan **21** 1765 (1966).
- ⁷ F. Hache, D. Ricard, and C. Flytzanis, J. Opt. Soc. Am. B **3** 1647 (1986).
- ⁸ G. S. Agarwal and S. D. Gupta, Phys. Rev. A **38** 5678 (1988).
- ⁹ L. Yang, K. Becker, F. M. Smith, R. H. Magruder, R. F. Haglund, L. Yang, R. Dorsinville, R. R. Alfano, and R. A. Zuhr, J. Opt. Soc. Am. B **11** 457 (1994).
- ¹⁰ T. Tokizaki, A. Nkamura, S. Kaneko, K. Uchida, S. Omi, H. Tanji, and Y. Asahara, Appl. Phys. Lett. **65**, 941 (1994).
- ¹¹ T. W. Roberti, B. A. Smith, and J. Z. Zhang, J. Chem. Phys. **102**, 3860 (1995).
- ¹² J.-Y. Bigot, J.-C. Merle, O. Cregut, and A. Daunois, Phys. Rev. Lett., **75**, 4702 (1995).
- ¹³ T. S. Ahmadi, S. L. Logunov, and M. A. Elsayed, J. Phys. Chem. **100**, 8053 (1996).
- ¹⁴ M. Perner, P. Bost, G. von Plessen, J. Feldmann, U. Becker, M. Mennig, M. Schmitt, and H. Schmidt Phys. Rev. Lett. **78**, 2192 (1997).
- ¹⁵ M. Nisoli, S. Stragira, S. De Silvestri, A. Stella, P. Tognini, P. Cheyssac, and R. Kofman, Phys. Rev. Lett. **78**, 3575 (1997).
- ¹⁶ T. Klar, M. Perner, S. Grosse, G. von Plessen, W. Spirk, and J. Feldmann, Phys. Rev. Lett. **80**, 4249 (1998).
- ¹⁷ T. V. Shahbazyan, I. E. Perakis, and J.-Y. Bigot, Phys. Rev. Lett. **81**, 3120 (1998).
- ¹⁸ W. S. Fann, R. Storz, and H. W. K. Tom, Phys. Rev. B **46**, 13 592 (1992).
- ¹⁹ C. K. Sun, F. Vallée, L. H. Acioli, E. P. Ippen, and J. G. Fujimoto, Phys. Rev. B **50**, 15 337 (1994).
- ²⁰ R. H. M. Groeneveld, R. Sprik, and A. Lagendijk, Phys. Rev. B **51**, 11 433 (1994).
- ²¹ N. Del Fatti, R. Bouffanais, F. Vallée, and C. Flytzanis, Phys. Rev. Lett. **81**, 922 (1998).
- ²² R. D. Averitt, S. L. Westcott, and N. J. Halas Phys. Rev. B **58**, 10 203 (1998).
- ²³ E. D. Belotskii, S. N. Luk'yanets, and P. M. Tomchuk, Zh. Eksp. Teor. Fiz. **101**, 163 (1992) [Sov. Phys. JETP **74**, 88 (1992)].
- ²⁴ D. S. Chemla, *Ultrafast Transient Nonlinear Optical Processes in Semiconductors in Nonlinear Optics in Semiconductors*, edited by R. K. Willardson and A. C. Beers (Academic Press, 1999).
- ²⁵ V. M. Axt and S. Mukamel, Rev. Mod. Phys. **70**, 145 (1998).
- ²⁶ J. Shah, *Ultrafast Spectroscopy of Semiconductors and Semiconductor Nanostructures* (Springer, New York, 1996).
- ²⁷ P. Kner, W. Schäfer, R. Löwenich, and D. S. Chemla, Phys. Rev. Lett. **81**, 5386 (1998).
- ²⁸ Th. Östreich, K. Schönhammer, and L. J. Sham, Phys. Rev. Lett. **74**, 4698 (1995); Phys. Rev. B **58**, 12920 (1998).
- ²⁹ V. Chernyak, S. Yokojima, T. Meier, and S. Mukamel Phys. Rev. B **58**, 4496 (1998).

- ³⁰ I. E. Perakis and D. S. Chemla, Phys. Rev. Lett. **72**, 3202 (1994); I. E. Perakis, Chem. Phys. **210**, 259 (1996).
- ³¹ T. V. Shahbazyan, N. Primožich, D. S. Chemla, and I. E. Perakis, Preprint, 1999.
- ³² The effects of the spill out of the electron wave-functions beyond the nanoparticle classical boundary were discussed, e.g., in V. V. Krezin, Phys. Rep. **220**, 1 (1992).
- ³³ U. Sivan, Y. Imry, and A. G. Aronov, Europhys. Lett. **28**, 115 (1994).
- ³⁴ D. Pines and P. Nozieres, *The theory of quantum liquids*, (W. A. Benjamin, Inc., New York, 1966), Vol. I.
- ³⁵ In semiconductor quantum dots, where the discrete energy levels are well resolved, the quasiparticle scattering rate is similar to that in the bulk only for energies larger than some critical energy; see, e.g., B. I. Altshuler, Y. Gefen, A. Kamenev, and L. S. Levitov, Phys. Rev. Lett. **78**, 2803 (1997).
- ³⁶ A. A. Lushnikov and A. J. Simonov, Z. Phys. **270**, 17 (1974).
- ³⁷ See, e.g., G. D. Mahan, *Many-Particle Physics* (Plenum, New York, 1990).
- ³⁸ In very small particles, the difference in the positions of the effective boundaries for the conduction and d -band densities leads to a shift in the linear absorption peak; see A. Liebsch, Phys. Rev. B **48**, 11 317 (1993); V. V. Krezin, Phys. Rev. B **51**, 1844 (1995).
- ³⁹ S. Ogawa, H. Nagano, and H. Petek, Phys. Rev. B **55**, 10 869 (1997).
- ⁴⁰ H. Ehrenreich and H. R. Philipp, Phys. Rev. **128**, 1622 (1962).
- ⁴¹ The notion of a time-dependent absorption coefficient can also be extended to the coherent regime, see I. E. Perakis, I. Brener, W. H. Knox, and D. S. Chemla, J. Opt. Soc. Am. B **13**, 1313 (1996).
- ⁴² G. L. Easley, Phys. Rev. B **33**, 2144 (1986).

FIGURES

FIG. 1. Calculated absorption spectra at positive time delays for nanoparticles with (a) $R = 5$ nm, (b) $R = 2.5$ nm, and (c) $R = 1.2$ nm.

FIG. 2. Calculated differential transmission spectra at positive time delays for nanoparticles with (a) $R = 5$ nm, (b) $R = 2.5$ nm, and (c) $R = 1.2$ nm.

FIG. 3. Temporal evolution of the differential transmission at frequencies close the SP resonance for nanoparticles with (a) $R = 5$ nm, (b) $R = 2.5$ nm, and (c) $R = 1.2$ nm. (d) Time-resolved pump-probe signal from Ref. 12.

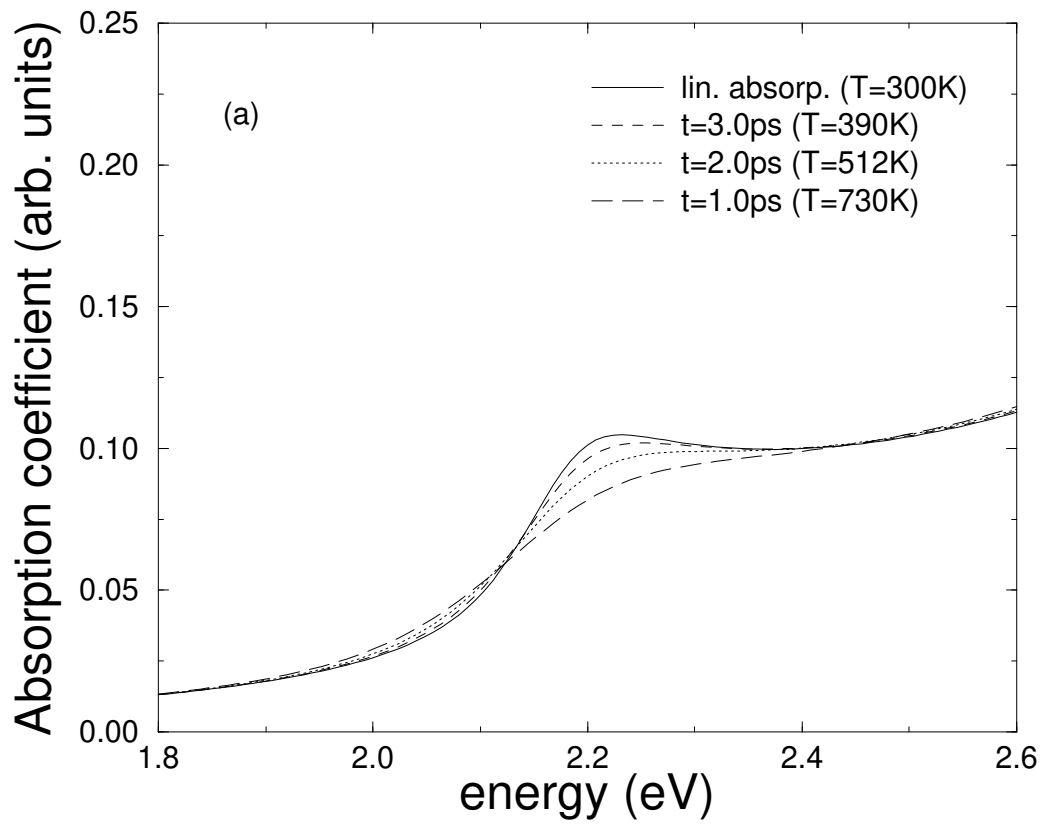


FIG. 1

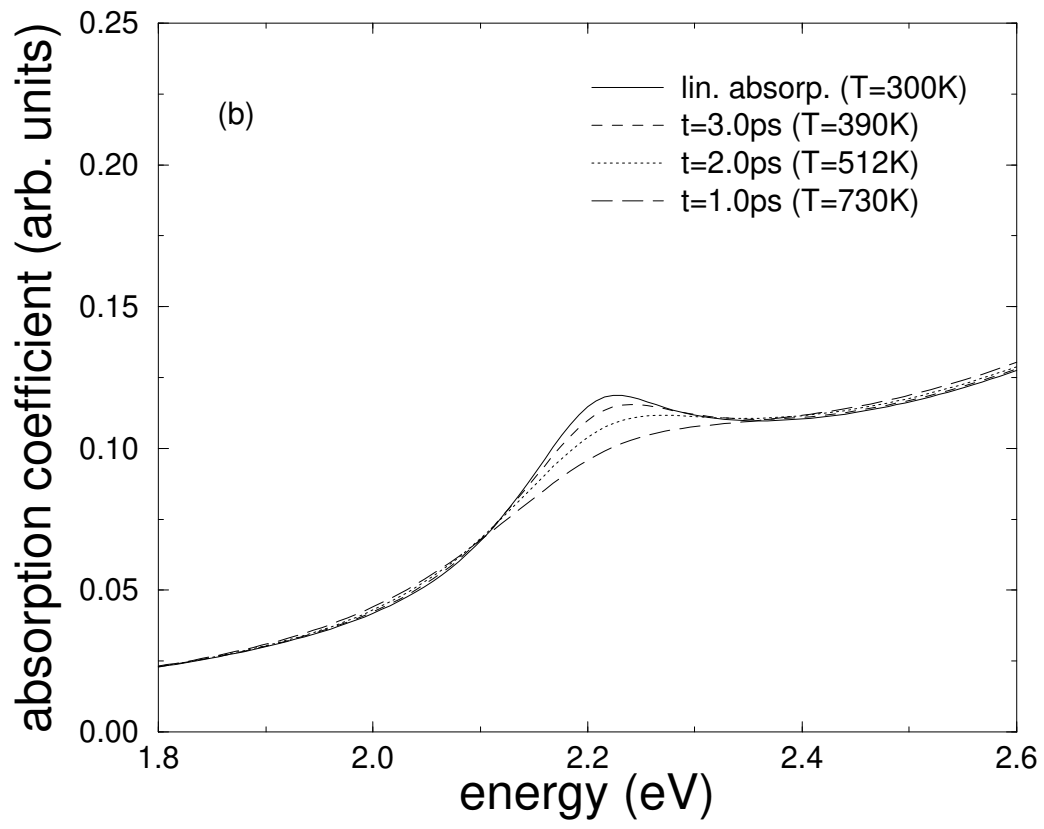


FIG. 1

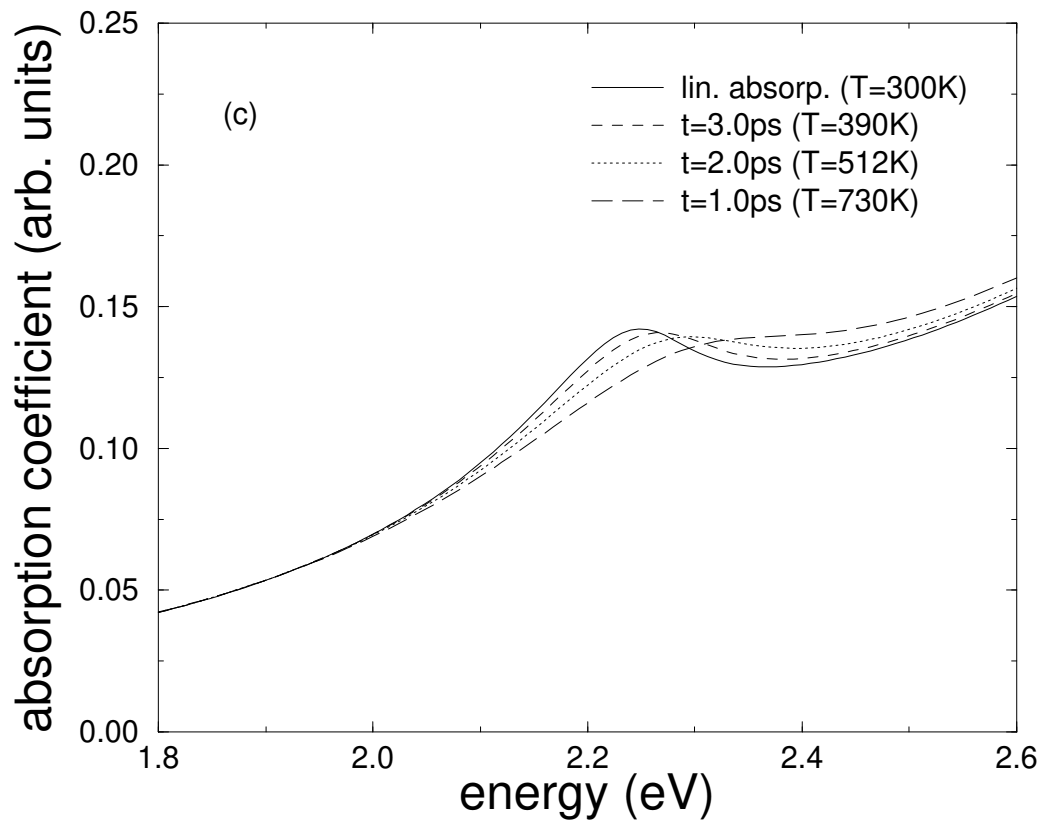


FIG. 1

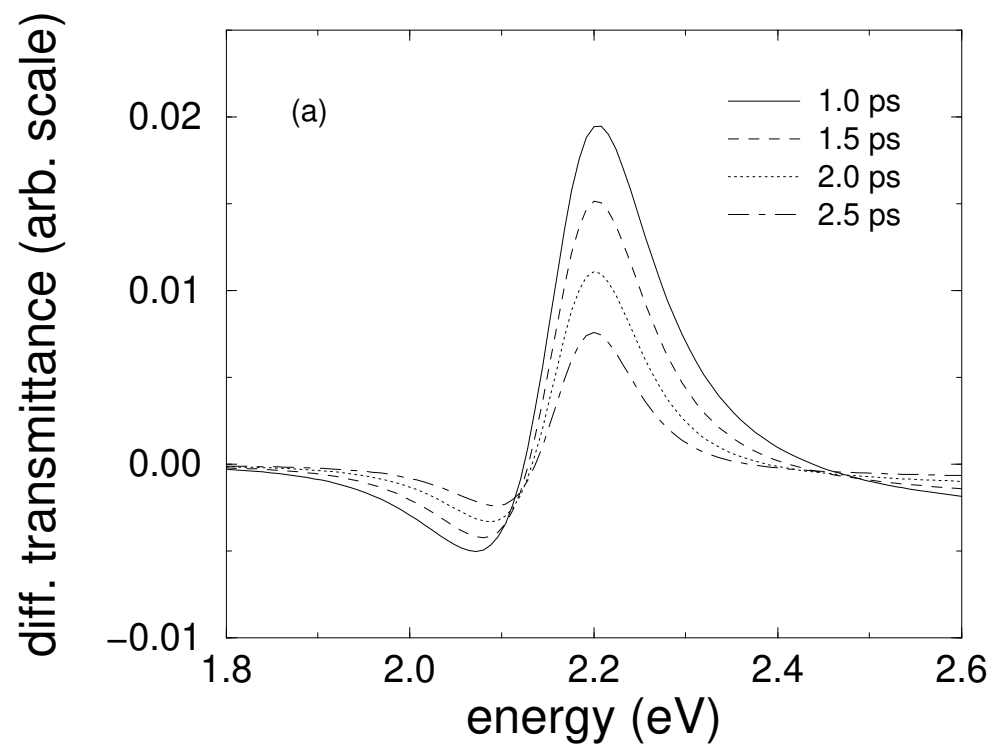


FIG. 2

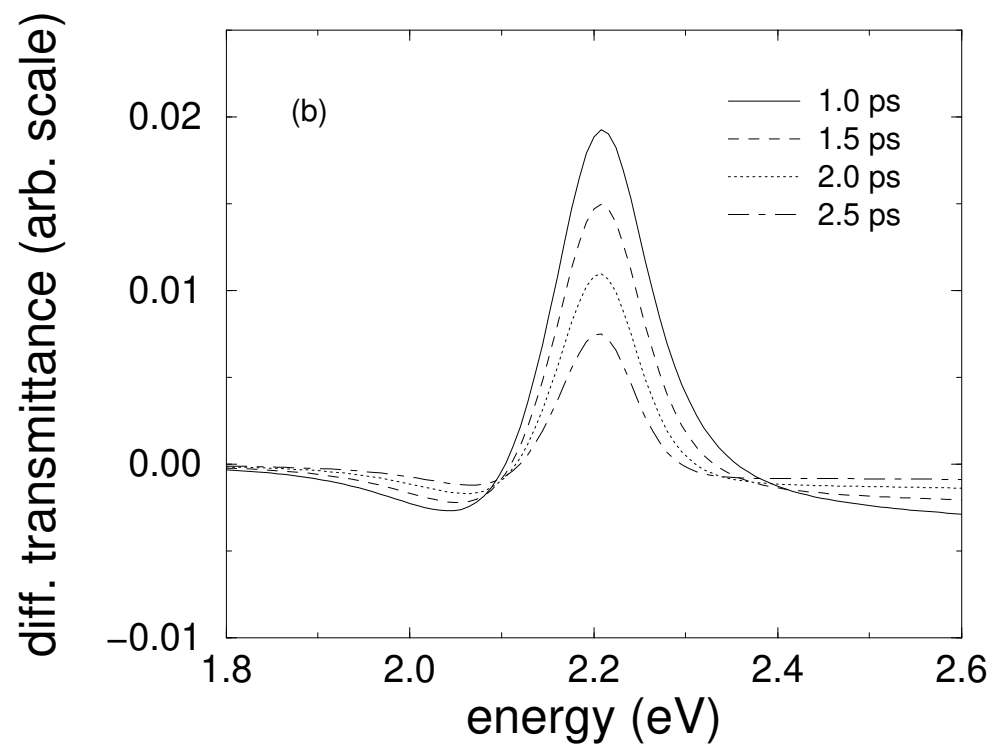


FIG. 2

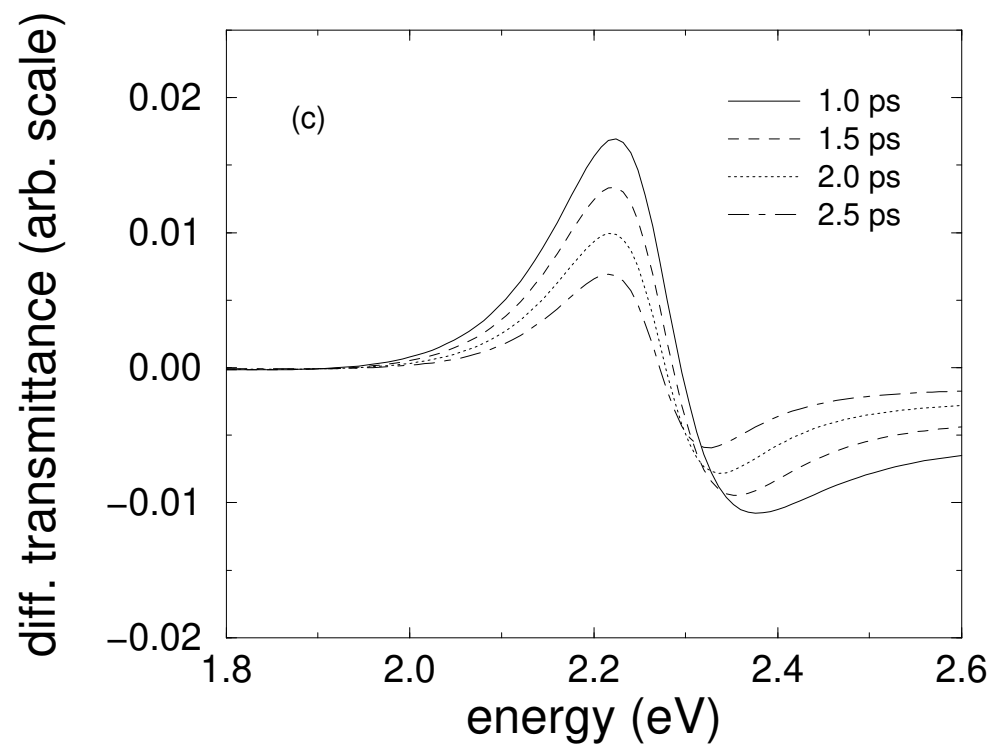


FIG. 2

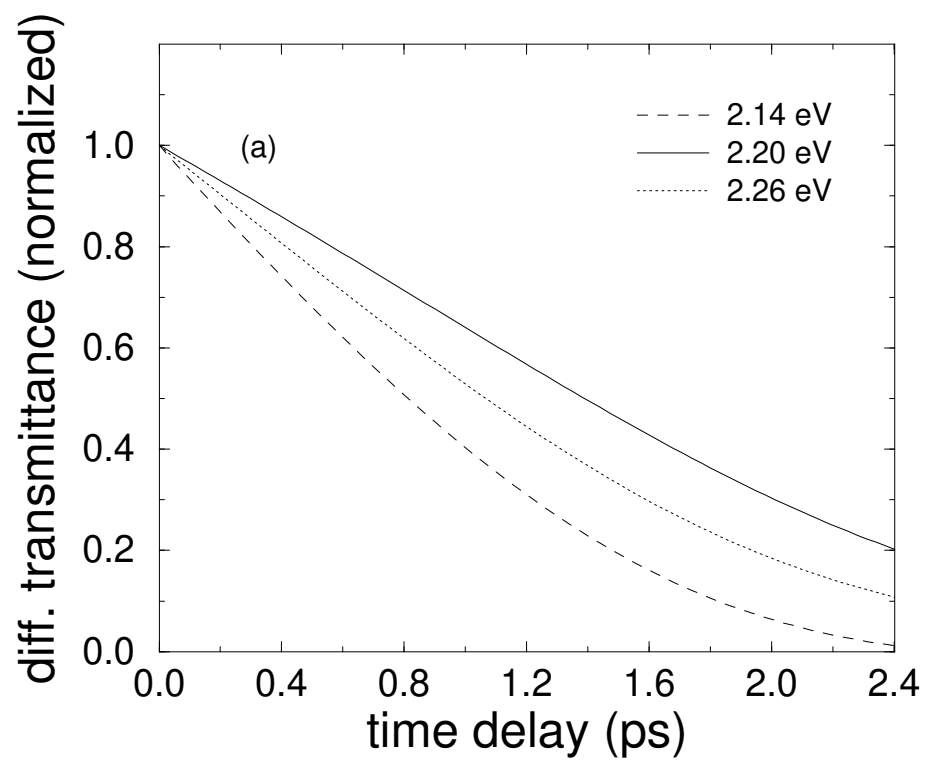


FIG. 3

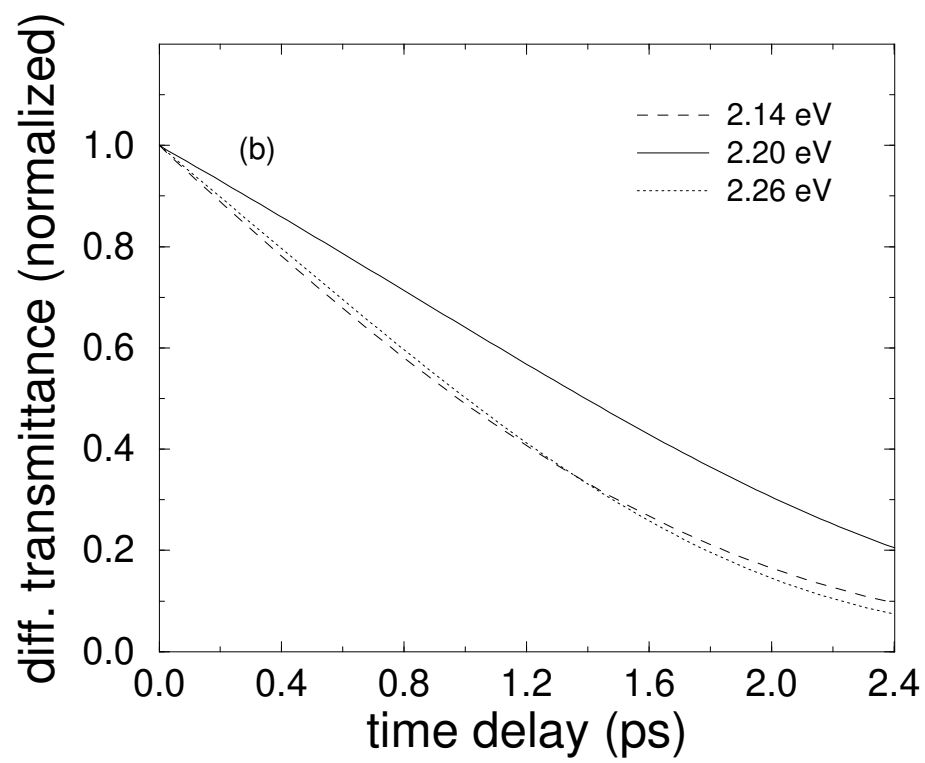


FIG. 3

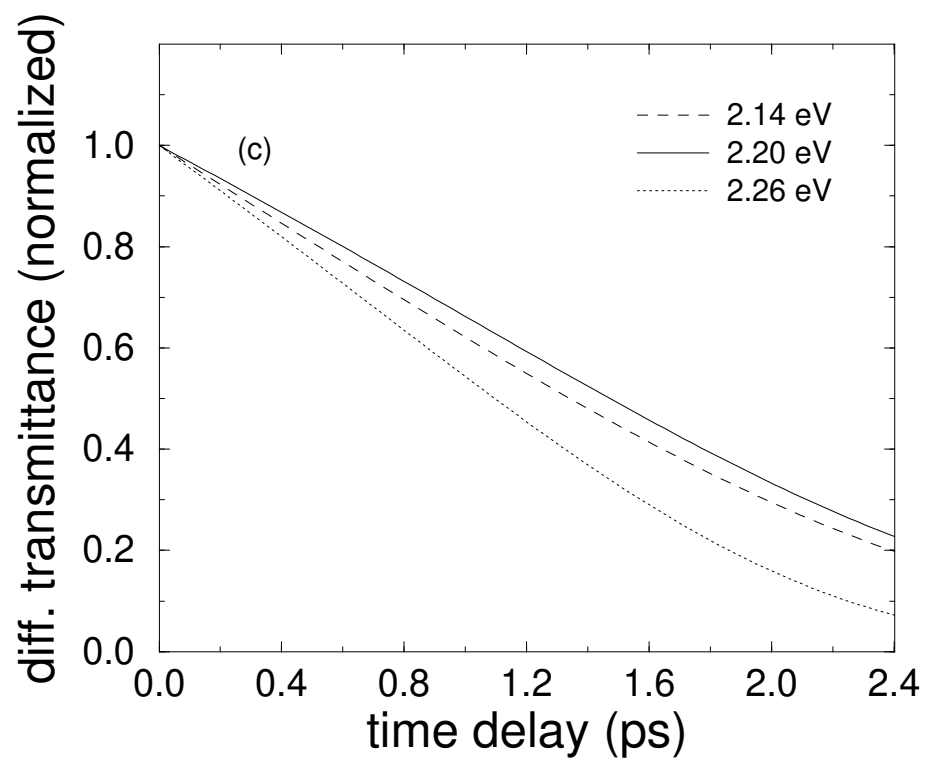


FIG. 3

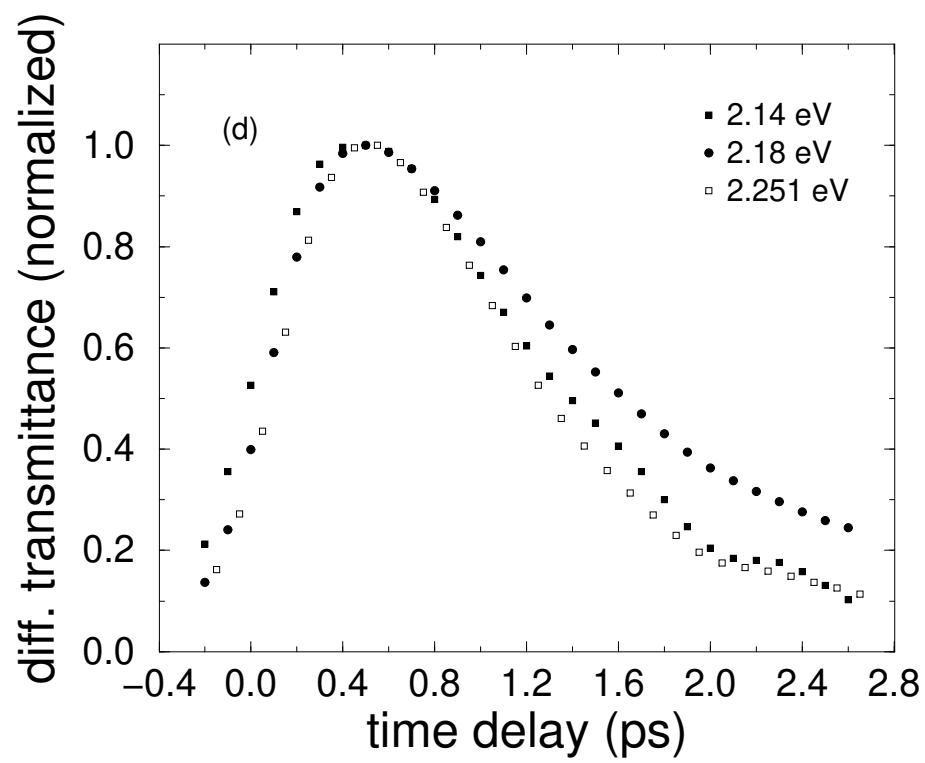


FIG. 3